

Compressive strength of fly ash magnesium oxychloride cement containing granite wastes

Ying Li^{a,c}, Hongfa Yu^{a,b,*}, Lina Zheng^{a,c}, Jing Wen^{a,c}, Chengyou Wu^{a,c}, Yongshan Tan^{a,c}

^a Qinghai Institute of Salt Lakes, Chinese Academy of Sciences, No. 18, Xinning Road, Xining 810008, PR China

^b Department of Civil Engineering, Nanjing University of Aeronautics and Astronautics, No. 29, Yudao Street, Nanjing 210016, PR China

^c The Graduate University of Chinese Academy of Sciences, No. 19, Yuquan Road, Beijing 100049, PR China

HIGHLIGHTS

- ▶ Granite waste and fly ash are incorporated into magnesium oxychloride cement (MOC).
- ▶ The water absorption of granite waste from the slurry results in increased hydration product of $5\text{Mg}(\text{OH})_2\cdot\text{MgCl}_2\cdot 8\text{H}_2\text{O}$.
- ▶ The excess water absorption of granite waste from low-concentration brine leads to compact microstructure of GFMOc, whereas from the high concentration of brine leads to porous microstructure.
- ▶ The sound composition and compact microstructure of the hydration product lead to high compressive strength of GFMOc.
- ▶ Incorporated granite waste can increase the compressive strength of fly ash MOC.

ARTICLE INFO

Article history:

Received 10 January 2012

Received in revised form 23 May 2012

Accepted 4 June 2012

Available online 13 September 2012

Keywords:

Magnesium oxychloride cement (MOC)

Fly ash

Granite waste

Compressive strength

ABSTRACT

This paper presents the results of an experimental investigation on compressive strength of granite waste fly ash magnesium oxychloride cement (GFMOc). Various GFMOc specimens were prepared with 23°Bé or 25°Bé brine and different proportions of granite fragment (GF) or granite sludge (GS) ranging from 0% (for the control mixture) to 40% of magnesia weight. Compression tests were conducted at the age of 3, 7, and 28 days. The hydration products and paste microstructure were analyzed by XRD and SEM, respectively. The results demonstrated that the water absorption and filling role of the fine particles of granite waste in GFMOc slurry are favorable for $5\text{Mg}(\text{OH})_2\cdot\text{MgCl}_2\cdot 8\text{H}_2\text{O}$ (P5) and dense microstructure, respectively. The quantity ratio of P5 to $\text{Mg}(\text{OH})_2$ (MH) and microstructure are important factors responsible for the compressive strength of GFMOc. The incorporation of granite wastes as aggregate can increase the compressive strength of fly ash magnesium oxychloride cement (FMOC).

© 2012 Published by Elsevier Ltd.

1. Introduction

Magnesium oxychloride cement (MOC) is an air-dried, magnesia-based cementitious material developed not long after the invention of Portland cement (PC) [1]. MOC is used extensively in residential and industry applications due to its advanced performance compared with PC. The characteristics of quick hardening and high early strength make MOC an ideal material for quick repairs [2]. Due to its qualities of fire resistance, low thermal conductivity, and good resistance to abrasion, MOC is commonly used for door frames [3], beams [4], fireproof materials [5], thermal

insulation materials [6], floor tiles [7,8], and grinding wheels [9,10], among others. MOC is also suitable for incorporation in a variety of organic and inorganic aggregates, which enables it to be able to solidify municipal waste [7] and fix sewage sludge [11]. The ability of MOC to manage solid wastes facilitates recycling and reduces the cost of MOC products.

MOC is obtained by mixing magnesia powder with brine (magnesium chloride solution). MOC is a by-product of hardened neat cement slurry of the $\text{MgO}\text{--}\text{MgCl}_2\text{--}\text{H}_2\text{O}$ ternary system; however, it has high water solubility and bad dimensional instability [2,12,13]. It is necessary to add various additives and fillers into the MOC neat cement slurry to improve water resistance and to avoid expansion-related problems [2–4,14]. For instance, the addition of a small quantity (for example, 1% by weight of magnesia) of phosphoric acid or soluble phosphates ($\text{NaH}_2\text{PO}_4\cdot 2\text{H}_2\text{O}$ or $\text{NH}_4\text{H}_2\text{PO}_4$) can greatly improve the water resistance of MOC [14]. According to Li et al. [2], the incorporation of fly ash into

* Corresponding author at: Qinghai Institute of Salt Lakes, Chinese Academy of Sciences, No. 18, Xinning Road, Xining 810008, PR China. Tel.: +86 25 8489 5233; fax: +86 25 8489 1754.

E-mail addresses: setdownly@126.com (Y. Li), yuhongfa@nuaa.edu.cn (H. Yu).

MOC can enhance the workability or fluidity, retard the setting time, and improve the water resistance while unexpectedly reducing the final compressive strength of the MOC mortars. In the MOC mortars, the more fly ash is added, the lower the compressive strength [2]. The compressive strength of MOC mortar has been found to decrease by about 35% when 30% of fly ash by weight of magnesia is incorporated [2]. However, there has been no explanation why this phenomenon happens [2]. Obviously, the physical and chemical properties of MOC, such as compressive strength, volume stability, and water resistance, are modified by various chemical or/and physical effects of the additives and fillers in the hydration processes.

Granite have diverse applications because of its versatile characteristics, such as high durability and resistance to scratches, stains, cracks, spills, heat, cold, and moisture. Unfortunately, a considerable and increasing amount of solid wastes from granite industries are generated in cutting and polishing [15]. These wastes are currently disposed in landfills with increasing cost and negative environmental impact, which affects the economic and environmental sustainability of such industrial productions, as well as public health [16].

In recent decades, environmental considerations have become a main concern, and efforts to reuse granite wastes have been undertaken. A number of previous studies have shown that granite residues have high potential as raw materials in the ceramic industry [15,17–19] and as aggregates in the building material industry [20–22]. For example, red clay roof tiles incorporated with granite wastes can reduce water absorption without increasing sintering temperature and pyroplastic deformation [15]. According to Binici et al. [20], granite residues as aggregates can be applied to improve the mechanical properties, workability, and chemical resistance of conventional concrete mixtures. Granite wastes are effective fillers and pozzolanic materials for mortars and concrete due to the ability to ameliorate the mechanical properties and corrosion resistance of mortars and concrete by improving compactness [20,21]. To the best of our knowledge, however, the effect of incorporating granite wastes into MOC has not been reported in recent literature.

Taking into account all the above-mentioned factors, this paper is dedicated to the investigation of the incorporation of granite wastes in fly ash magnesium oxychloride cement (FMOC) formulations. The effects of brine concentration, granite waste amount, and particle size distribution (PSD) on the compressive strength, hydration products, and microstructure of granite waste fly ash magnesium oxychloride cement (GFMO) are discussed in detail. The final objective of this work is to examine the feasibility of using granite wastes as aggregate to improve the compressive strength of FMOC.

2. Experiments

2.1. Raw materials

2.1.1. Light-burnt magnesia

The light-burnt magnesia used in this experiment was produced by Haicheng Magnesium Cement Mining, Ltd. (Liaoning Province, China). The active MgO, which hydrated at 105 °C and 101.3 kPa [23], was 60.0% by weight. The chemical compositions of the light-burnt magnesia by X-ray fluorescence (XRF, Axios PW4400) are summarized in Table 1 and the mineralogical compositions are shown in Fig. 1 by X-ray diffraction (XRD, PANalytical X'PRO Pert). The light-burnt magnesia mixture contains magnesia, magnesite, and minor amounts of quartz and calcite. The crystalline phases identified by XRD are in accordance with the results obtained by XRF (Table 1).

Table 1
Chemical compositions of the raw materials, as determined by XRF (wt.%).

	Al ₂ O ₃	SiO ₂	MgO	Fe ₂ O ₃	CaO	Na ₂ O	K ₂ O	Others
Magnesia	0.15	6.07	80.20	0.41	1.30	–	–	11.87
Fly ash	37.70	49.90	0.54	4.38	3.74	–	–	3.74
Granite sludge	10.42	57.58	0.58	2.06	1.85	3.29	3.42	20.80

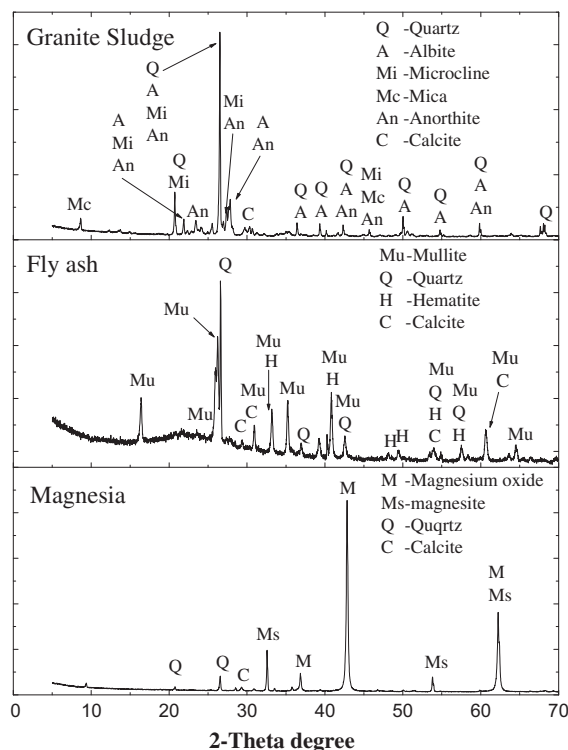


Fig. 1. XRD pattern of the raw materials (Cu K α radiation at 40 kV/30 mA, scan rate: 0.02°/s).

2.1.2. Brine

The brine was prepared by dissolving bischofite in tap water. The bischofite was produced by Jiayoumeiye, Ltd. (Qinghai Province, China) with 98.4% purity.

2.1.3. Fly ash

Fly ash is commonly used as aggregate in MOC [2,3]. In this experiment, 20% fly ash (by weight of light-burnt magnesia) was added into the GFMO specimens to improve the workability and water resistance of the MOC mortars [2]. However, the workability and water resistance of GFMO are not reported in this paper. The chemical and mineralogical compositions of fly ash are shown in Table 1 and Fig. 1, as detected by XRF and XRD, respectively. The result of XRF shows that fly ash mainly consists of SiO₂ (49.90%) and Al₂O₃ (37.70%), together with secondary amounts of Fe₂O₃, CaO, and MgO. The mineralogical compositions of fly ash are mullite and quartz mixed with a small quantity of hematite and calcite. The chemical compositions obtained by XRF are in line with the mineralogical compositions by XRD.

2.1.4. Granite waste

Granite fragments (GF) from sawing the block and granite sludge (GS) from polishing the slab were supplied by Lindun Quarry of Changtai County (Fujian Province, China). The as-received GS containing about 40% moisture was sun-dried. The dried GS's

chemical compositions analyzed by XRF and the mineralogical characterizations detected by XRD are shown in Table 1 and Fig. 1, respectively. As shown in Table 1, GS has a high proportion of SiO₂ (57.58%) and Al₂O₃ (10.42%). Other non-negligible components include K₂O (3.42%), Na₂O (3.29%), and Fe₂O₃ (2.06%). Fig. 1 shows that the GS is primarily composed of quartz and albite with minor amounts of microcline, mica, anorthite, and calcite. The identified crystalline phases are matched by the results observed by XRF.

The particle size distribution (PSD) of granite waste was determined by cement standard sieves that conformed to Chinese National Standard GB/T 14684-2001 and laser scattering particle analyzer (LSPA, Mastersizer 2000). The GF particles screened at 0.15, 0.30, 0.60, 1.18, 2.36, and 4.50 mm standard sieve were 30.84%, 10.98%, 16.44%, 12.28%, 12.62%, and 16.12% by weight, respectively. Particle finer than 0.15 mm in GF were further analyzed by LSPA. The results of LSPA revealed that this powder has a high specific surface area of 546 m²/Kg and a PSD with a mean value of 71 μm, a D₁₀ of 5.4 μm, a D₅₀ of 49.6 μm, and a D₉₀ of 167.6 μm. GS powder has higher specific surface area of 748 m²/Kg and PSD with a mean value of 28.4 μm and a D₁₀ of 4.6 μm, a D₅₀ of 20.5 μm, and a D₉₀ of 53.5 μm, which were also analyzed by LSPA.

2.2. Specimen preparation

Based on previous studies [24,25], the molar ratio of active MgO to MgCl₂ (MgO_a/MgCl₂) was kept constant at 7 and the concentrations of brine were 23°Bé (molar ratio of H₂O/MgCl₂ was 19.6, ρ was 1.19 g/mL, and w was 21.2%) and 25°Bé (molar ratio of H₂O/MgCl₂ was 17.3, ρ was 1.21 g/mL, and w was 23.4%) in this experiment. The contents of GF or GS were 10%, 20%, 30%, and 40% by the weight of light-burnt magnesia in the specimens. In each batch of specimens, the dosages of the recipes are presented in Table 2. C3 and C5 are the control specimens. In Table 2, the V/m, the volume (mL) of the brine to the mass (g) of the light-burnt magnesia, was calculated as follows:

$$\frac{V}{m} = \frac{M_1 w_2}{M_2 n \rho w_1} \quad (1)$$

where V is the volume (mL) of the brine, m is the weight (g) of the light-burnt magnesia, M₁ is the molecular weight (g/mol) of MgCl₂, w₂ is the content (%) of active MgO in the light-burnt magnesia, M₂

is the molecular weight (g/mol) of MgO, n is the MgO_a/MgCl₂, ρ is the density (g/mL) of brine, and w₁ is the mass fraction (%) of MgCl₂ in the brine.

Light-burnt magnesia, fly ash, and granite waste were mixed thoroughly, and then brine was added to the blended powder. It was then mixed for about a few minutes to produce GFMOCC cement. For each mixture assigned in Table 2, bar specimens with size of 40 mm × 40 mm × 160 mm were cast in stainless steel molds through vibration compaction. Each mixture was then sealed with polyethylene film and air cured at a temperature of 23 ± 2 °C and 60 ± 5% humidity. After 24 h, the resultant specimens were released from the mold and cured at room temperature.

For convenience, the following abbreviation will be used to specify the different recipes of each mixture. A mixture with concentration of brine 20 + x (x = 3 and 5) °Bé and 10 × y (y = 1, 2, 3, and 4)% GF will be designated as Fxy. Similarly, “S” in “Sxy” means that GS was used as an aggregate. For instance, F31 indicates that the specimen consists of 23°Bé brine and 10% GF, and S54 consists of 25°Bé brine and 40% GS.

2.3. Specimen analysis

2.3.1. Compressive strength analysis

Uniaxial compression strength was tested using a concrete compression machine (TYE-300) with a maximum load of 300 kN. At the age of 3, 7, and 28 days, the compressive strengths were measured at a loading rate of 2400 N/s as per Chinese National Standard GB/T17671-1999. The results were presented as the average of six replicates.

2.3.2. XRD and SEM

The crystalline phases of the GFMOCC pastes after the 28-day curing were identified by XRD patterns. The powder samples were prepared by crushing the specimens and passing the powder through a sieve with a screen aperture of 75 μm. Rietveld method was employed to perform qualitative analysis [26,27] using Topas 3.0 software [28].

The microstructure of the GFMOCC pastes after the 28-day curing were characterized by scanning electron microscopy (SEM, JSM-5610LV) on a fractured surface with gold coating.

3. Results

Compressive strength is one of the important indices to evaluate product quality in the application of cementitious material [19]. The measured 3-day, 7-day, and 28-day compressive strengths of the GFMOCC specimens with various percentages of granite waste are shown in Fig. 2. The dashed lines in the figures stand for the compressive strength of the control mixture.

3.1. The effect of brine concentration

From the test results in Fig. 2, it is shown that the higher concentration of brine is used, the higher the compressive strength of the GFMOCC. The compressive strengths of GFMOCC specimens mixed with high concentration of brine (25°Bé, F5y series) are higher than the specimens with low concentration of brine (23°Bé, F3y series) at the same amount of GF and curing age. For instance, the compressive strengths of F5y specimens separately show 24.8%, 24.1%, 16.9%, and 16.0% higher than those of F3y specimens in the order of increased GF ratio from 10% to 40% at the age of 28 days. The compressive strengths of S5y series specimens are also higher than those of S3y series. The compressive strength of S54 is 101.4% and 103.2% as high as that of S34 at 3 days and 28 days, respectively. However, it is an exception that the com-

Table 2
The recipes of GFMOCC specimens.

No.	Brine (°Bé)	V/m ^a (mL/g)	Fly ash ^b (%)	GF ^b (%)	GS ^b (%)
F31	23	0.81	20	10	0
F32	23	0.81	20	20	0
F33	23	0.81	20	30	0
F34	23	0.81	20	40	0
F51	25	0.72	20	10	0
F52	25	0.72	20	20	0
F53	25	0.72	20	30	0
F54	25	0.72	20	40	0
S31	23	0.81	20	0	10
S32	23	0.81	20	0	20
S33	23	0.81	20	0	30
S34	23	0.81	20	0	40
S51	25	0.72	20	0	10
S52	25	0.72	20	0	20
S53	25	0.72	20	0	30
S54	25	0.72	20	0	40
C3	23	0.81	20	0	0
C5	25	0.72	20	0	0

^a The volume (mL) of the brine to the mass (g) of the light-burnt magnesia.

^b By the weight of light-burnt magnesia.

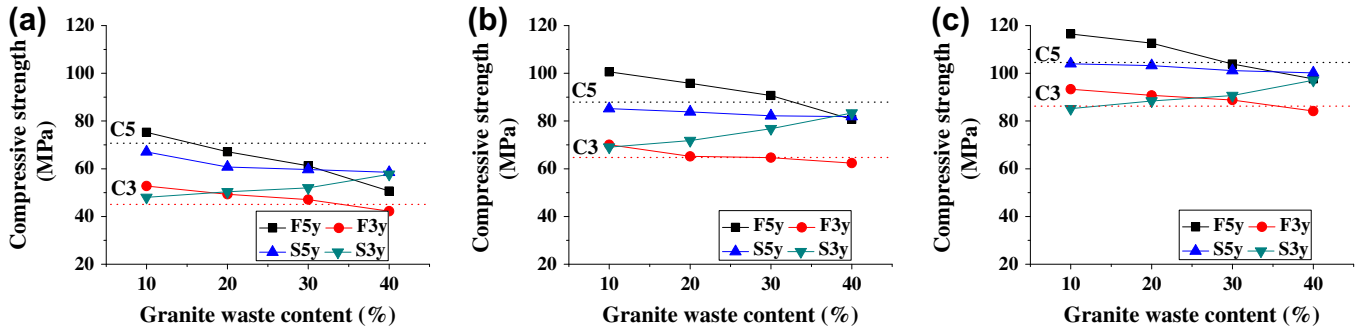


Fig. 2. Compressive strength as a function of percentages of granite rejects. (a) 3-day, (b) 7-day, and (c) 28-day; F5y: mixed GF with 25°Bé brine; F3y: mixed GF with 23°Bé brine; S5y: mixed GS with 25°Bé brine; S3y: mixed GS with 23°Bé brine; y = 1, 2, 3, and 4.

pressive strength of S54 (81.8 MPa) is slightly lower than 83.4 MPa of S34 at 7 days.

3.2. The effect of amount of granite waste

Fig. 2 illustrates that with the increase of granite waste content ranging from 0% to 40%, three variations in the compressive strength of GFMOc specimens are presented as follows: (1) increasing first then decreasing, (2) slightly decreasing, and (3) constantly increasing.

From the plots in Fig. 2, the compressive strengths of the Fxy series specimens decrease with an increase in the GF content from 10% to 40% at all ages. For the F3y series, the specimen with 10% GF (F31) shows compressive strengths 16.9%, 8.2%, and 8.2% higher than those of the control mixture (C3) for the 3-day, 7-day and 28-day curing. However, the specimen with 40% GF (F34) shows lower compressive strengths throughout the test period, namely, 93.5%, 96.4%, and 97.6% of the control specimen at the ages of 3, 7, and 28 days, respectively.

For the F5y series, the compressive strength of the specimen with 10% GF (F51) shows 6.4%, 14.4%, and 12.8% higher than that of the control mixture (C5) at 3, 7, and 28 days, yet the specimen with 40% GF (F54) is 28.4%, 8.2%, and 5.4% lower than those of C5, respectively. These results are consistent with other findings that the use of granite wastes in concrete would lead to increased compressive strength at low content and decreased compressive strength at high content [21,22,29].

In Fig. 2, the compressive strengths of the S5y series specimens show lower strength than that of the control mixture (C5) and slightly reduce by the increase in the GS ratio. The compressive strength of specimen with 10% GS (S51) is 5.1%, 3.1%, and 0.5% lower and the specimen with 40% GS (S54) is 17.3%, 6.9%, and 4.2% lower than those of C5 at the 3, 7, and 28 days, respectively.

From Fig. 2, the compressive strengths of the S3y series specimens exhibit an increasing trend at all ages with the increase in GS content. The specimen with 10% GS (S31) indicates compressive strengths of 106.4%, 107.5%, and 98.8% as high as the control mixture (C3) at 3-day, 7-day, and 28-day, whereas the specimen with 40% GS (S34) is 127.9%, 129.8%, and 112.6% of C3, respectively.

3.3. The effect of particle size of granite waste

Fig. 2 also displays the effects of particle size of granite waste on the compressive strength of GFMOc. For the GFMOc specimens with 23°Bé brine, the compressive strength of the specimen with GS (S31) is lower than that of the specimen with GF (F31) when the content of granite waste content is 10% at all the ages. The compressive strengths of GS specimens, however, are higher than those of GF specimens when the content of granite waste is no less than 30% at 3-day, 7-day, and 28-day curing.

For the GFMOc specimen incorporated with 25°Bé brine, the compressive strengths of samples show the similar tendency as seen from the 23°Bé specimens at all the ages. The specimens with no more than 30% GS (S51, S52, and S53) yield lower compressive strengths than those with GF (F51, F52, and F53). The phenomenon is adverse when the specimen includes 40% granite residues. S54 shows higher compressive strength than F54. In a word, the compressive strengths of GFMOc specimens incorporated with low content (such as 10%) of GF are higher than that of GS, whereas mixed with high content (such as 40%) of GF are lower than that of GS at all ages.

3.4. XRD and SEM

The crystalline phases of the GFMOc pastes at the 28 days, as identified by XRD, are shown in Fig. 3. The quantities of the mineralogical compositions are also presented in Table 3, which have been analyzed by Rietveld method [26,27]. Fig. 3 displays that the specimens with 30% GS and the control samples at the 28-day curing are primarily composed of the hydration products of 5 Mg(OH)₂·MgCl₂·8H₂O (Phase 5 or P5), brucite (Mg(OH)₂ or MH), and minor amounts of magnesite, quartz, and magnesia that originated from the raw materials (the former also contains albite from GS). The results from XRD do not indicate that GS yields new hydration products in MOc.

The results in Table 3 also show that the mixtures with 25°Bé brine (C5 and S53) generate more P5 and less MH than that with 23°Bé brine (C3 and S33). Moreover, the quantity ratios of P5 to MH (P5/MH ratio) in specimens with GS (S33 and S53) are greater than those of the corresponding control mixture (C3 and C5), which demonstrates the generation of P5 and the restraint of the hydration product of MH when GS is incorporated in the FMOC.

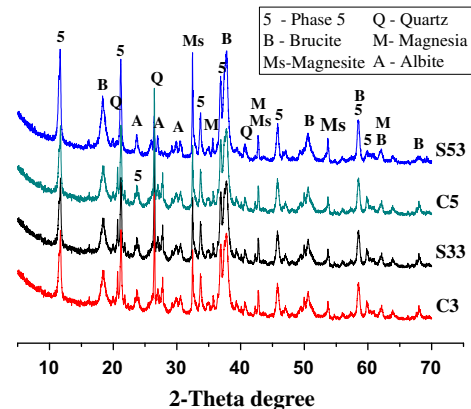


Fig. 3. XRD patterns of the GFMOc (S33 and S53) and the control mixture (C3 and C5) at the 28-day curing.

Table 3

The crystalline phases and their quantity of the specimens at the age of 28 days (wt.%).

	Phase 5	Brucite	Magnesite	Quartz	Magnesia	Albite	R ^a
C3	50.6	36.7	9.9	2.7	0.2	–	1.4
S33	46.9	31.8	4.6	7.8	3.3	5.5	1.5
C5	57.4	32.0	5.6	2.8	2.9	–	1.8
S53	51.7	27.1	3.8	7.5	4.4	5.4	1.9

^a R: the quantity ratio of Phase 5 to brucite (P5/MH ratio) in specimen at 28-day.

Fig. 4 illustrates the SEM micrographs of GF/MOC and the control pastes with a multiple of 100 times at 28 days. From the images, the control mixture with 23°Bé brine (C3, Fig. 4a) has a higher porous microstructure than the control mixture with 25°Bé brine (C5, Fig. 4b). When 30% GS is added to the specimen with 23°Bé brine (S33, Fig. 4c), the microstructure becomes more compact than the control mixture (C3). However, the situation is opposite for the specimen with 25°Bé brine (S53, Fig. 4d). The high porous microstructure is harmful for the strength of the GF/MOC specimen.

4. Discussion

P5 and MH are the major reaction products when $MgO_a/MgCl_2$ and $H_2O/MgCl_2$ are greater than 5 and 13 in MOC, respectively [24,30]. The former is responsible for the strength of MOC, but the latter has a negative effect on strength [12,31,32]. In the slurry of MOC, the higher concentration of brine is favorable for the P5, whereas the lower the more MH is produced [32]. Hence, the specimens with 25°Bé brine yield more P5 and less MH than the specimens with 23°Bé brine (Table 3). Meanwhile, the lower the concentration of brine, the more free water the MOC slurry contains. The free water that leads to formation the internal voids and capillary channels in the MOC specimens (Fig. 4a) causes a decline in its quality. Therefore, the compressive strengths of F5y and S5y series are higher than those of F3y and S3y series at the same curing age, respectively. This finding is consistent with what has been observed elsewhere [9,24,27,33].

GF grains with about 30.84% fine material by weight (less than 150 μm) are scattered between 5.4 μm and 4500 μm and have angular shapes [22]. The versatility of GF is favorable for compressive strength in many ways. First, the large surface area of the fine material (546 m^2/Kg) that absorbs plenty of free water results in brine concentrating, which causes a larger P5/MH ratio in GF/MOC than in the control mixture (Table 3). The finer particles (less than 60 μm [21]) then play an important role in changing the internal voids and capillary channels in the slurry, thus reducing the number of large ones [34]. This result is proven by the SEM micrograph of the pastes in Fig. 3a and c. Furthermore, the fine particles fill the gaps between the granular skeleton formed from the large granite leftover fragments to improve the particle packing density of the cementitious system [35,36], which is also beneficial for improving strength. The high angularity of the GF grain increases the bond between the particles and the cement paste that enhances the GF/MOC strength, which is in agreement with the finding that the angular but non-pozzolanic activity slag as an aggregate increases the compressive strength of concrete [37]. Therefore, the specimens with 10% GF yield higher strength than the reference samples.

On the other hand, the amounts of granite grains increase as increase of the GF ratio in GF/MOC. The fine and coarse aggregate particles need more P5 to be effectively coated, so high amounts of GF grains consequently lead to a decrease in compressive strength [29]. Hence, with the growing content of GF, the strengths of the F3y and F5y series specimens decrease obviously. Moreover, because of the weak and large interface between the fragment and the hydration product when the mixtures are incorporated with 40% GF, the specimens yield lower compressive strength than those with 40% GS.

Porosity is a key factor of strength in cementing material and high porosity weakens the bond between the concrete ingredients [38]. It is apparent that the surplus water in the slurry of C3 (Table 2) increases the porous microstructure (Fig. 4a). As mentioned above, when the finer GS particles (D_{90} of 53.5 μm) with greater specific surface (748 m^2/Kg) are added in the slurry with 23°Bé brine, they fill into the internal voids and capillary channels to decrease the number of large pores (Fig. 4c). They also absorb free

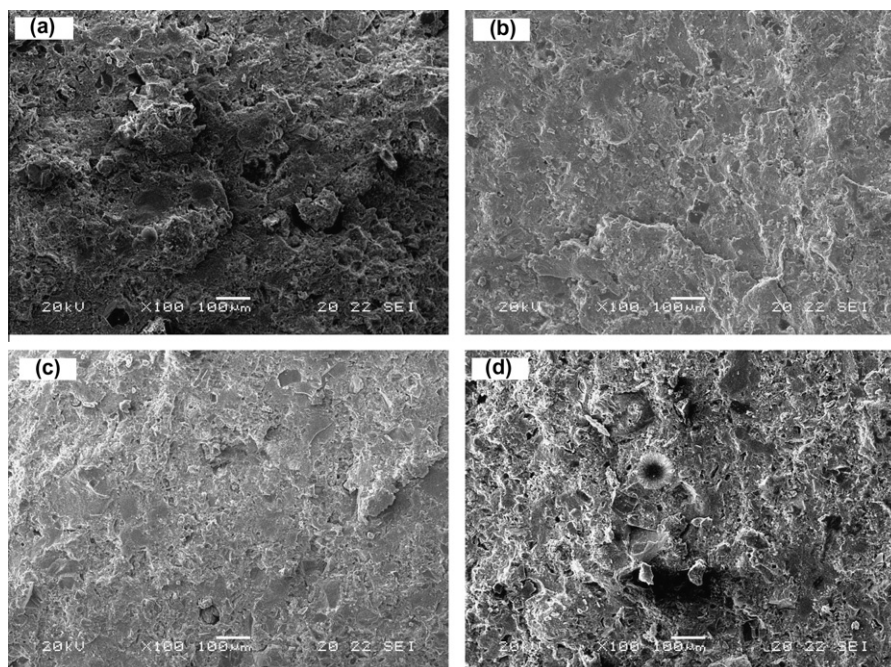


Fig. 4. SEM micrograph of the control samples and the specimens with 30% GS at 28 days. (a) C3, (b) C5, (c) S33, and (d) S53.

water to increase the P5/MH ratio (Table 3). Filling and absorption are functions of the percentages of the GS particles, such that the more GS particles are added, the more effective their roles become. Consequently, the compressive strengths of the S3y series GFMOc are higher than those of the control mixture (C3) and they increase as GS contents increase at all the ages. When the GS content reaches 50%, however, the fluidity of the slurry becomes too bad to mold.

Owing to the less free water in the slurry of C5 (Table 2), the microstructure of C5 at 28 days is denser than that of C3 (Fig. 4a and b). Nevertheless, when GS particles are added to the slurry with 25° Bé brine, the quantity of available water in the paste considerably reduces because of water absorption by the fine grains. In fact, the workability of S5y series slurry becomes poorer during mixing in the order of 10–40% GS. It results in a more porous microstructure in the specimens with the increasing content of GS. The increasing pore in the specimen leads to a reduction of the compressive strength of the S5y series specimens.

Fortunately, the fine grains absorbing water from the slurry increase brine concentration, leading to the production of more P5 and less MH. Thus, the P5/MH ratio of S53 specimen is higher than that of C5 in Table 3. The incremental P5 can counteract the harmful effect of porous microstructure to a certain extent. Therefore, the compressive strengths of the S5y series specimens slightly drop as the GS ratio increases. Moreover, a further increasing of the P5/MH ratio probably becomes the more decisive factor for the compressive strength of GFMOc than the dense microstructure. For this reason, the compressive strength of S53 is higher than that of S33 (Fig. 2) although the microstructure of S53 is more porous (Fig. 4c and d).

GS has pozzolanic activity based on its content in primary chemical components, such as SiO₂, Al₂O₃, and Fe₂O₃ (Table 1) [21,39]. However, GS has no pozzolanic effect in GFMOc from the XRD and compression tests. The possible reason is that the lower alkalinity of MOC (pH < 9.0 [40]) is not strong enough to activate the pozzolanic reactivity.

5. Conclusions

The following conclusions are drawn regarding the incorporation of granite waste with FMOC:

- The strong water absorption of the fine particles in granite waste, which concentrates the brine in the slurry of GFMOc, leads to an increase of P5/MH ratio and a following increased of compressive strength.
- The fine particles of granite waste play an important role in filling large pores and internal gaps in the slurry to generate a compact microstructure, which is beneficial for the increase of compressive strength.
- Both the P5/MH ratio and microstructure are important factors responsible for the compressive strength of GFMOc. The sound composition and the compact microstructure of the hydration product lead to high compressive strength of GFMOc. When GS is mixed with 23° Bé brine the compressive strength of GFMOc is higher than that of the corresponding FMOC. In other words, GS with a low concentration of brine (such as 23° Bé) can prevent the compressive strength from decreasing when fly ash is mixed with MOC [2]. The incorporation of small amounts of GF (such as 10%) can also increase the compressive strength of FMOC. However, GS is not suitable for the incorporation of high-concentration brine (such as 25° Bé) to increase the compressive strength of GFMOc due to both the strong water absorption of the fine particles of GS and few free water in the FMOC slurry.

Acknowledgements

The partial financial support from the One-Hundred Talent Project of CAS granted to HFY (B0210) and the Qinghai Province Science and Technology Tackling Key Project under Grant No. 2008-G-158 is greatly acknowledged. We thank Jinmei Dong and Junfang Cui (University College Dublin, Ireland) for their help in writing this paper, Weiwei Zhu (Southeast University, Nanjing, China) for her conscientious assistance in XRD qualitative analysis by Topas 3.0 software. We also thank three anonymous reviewers for very constructive comments and suggestions that have significantly improved the manuscript.

References

- [1] Sorrel S. On a new magnesium cement. *C R Acad Sci* 1867;65:102–4.
- [2] Chau CK, Chan J, Li ZJ. Influences of fly ash on magnesium oxychloride mortar. *Cem Concr Compos* 2009;31(4):250–4.
- [3] Zhou X, Li Z. Light-weight wood–magnesium oxychloride cement composite building products made by extrusion. *Constr Build Mater* 2012;27(1):382–9.
- [4] Plekhanova TA, Keriene J, Gailius A, Yakovlev GI. Structural, physical and mechanical properties of modified wood-magnesia composite. *Constr Build Mater* 2007;21(9):1833–8.
- [5] Montle JF, Mayhan KG. The role of magnesium oxychloride as a fire-resistive material. *Fire Technol* 1974;10(3):201–10.
- [6] Ji Y. Study of the new type of light magnesium cement foamed material. *Mater Lett* 2001;50(1):28–31.
- [7] Li GZ, Yu YZ, Li JQ, Wang YZ, Liu HS. Experimental study on urban refuse/magnesium oxychloride cement compound floor tile. *Cem Concr Res* 2003;33(10):1663–8.
- [8] Li J, Li G, Yu Y. The influence of compound additive on magnesium oxychloride cement/urban refuse floor tile. *Constr Build Mater* 2008;22(4):521–5.
- [9] Karimi Y, Monshi A. Effect of magnesium chloride concentrations on the properties of magnesium oxychloride cement for nano-SiC composite purposes. *Ceram Int* 2011;37(7):2405–10.
- [10] Ozturk A, Timucin M. Silicon carbide particle embedded magnesium oxychloride cement composite bricks for polishing of porcelain stoneware tiles. *Adv Appl Ceram* 2011;110(7):400–8.
- [11] Ma JL, Zhao YC, Wang JM, Li W. Effect of magnesium oxychloride cement on stabilization/solidification of sewage sludge. *Constr Build Mater* 2009;24(1):79–83.
- [12] Matkovic B, Young JF. Microstructure of magnesium oxychloride cements. *Nat Phy Sci* 1973;246(153):79–80.
- [13] Sorrell CA, Armstrong CR. Reactions and equilibria in magnesium oxychloride cements. *J Am Ceram Soc* 1976;59(1–2):51–4.
- [14] Deng DH. The mechanism for soluble phosphates to improve the water resistance of magnesium oxychloride cement. *Cem Concr Res* 2003;33(9):1311–7.
- [15] Torres P, Fernandes HR, Olhero S, Ferreira JMF. Incorporation of wastes from granite rock cutting and polishing industries to produce roof tiles. *J Eur Ceram Soc* 2009;29(1):23–30.
- [16] Mota R, Monteiro Santos FA, Mateus A, Marques FO, Gonçalves MA, Figueiras J, et al. Granite fracturing and incipient pollution beneath a recent landfill facility as detected by geoelectrical surveys. *J Appl Geophys* 2004;57(1):11–22.
- [17] Segadães AM, Carvalho MA, Acchar W. Using marble and granite rejects to enhance the processing of clay products. *Appl Clay Sci* 2005;30(1):42–52.
- [18] Menezes RR, Malzac HG, Santana LNL, Lira HL, Ferreira HS, Neves GA. Optimization of wastes content in ceramic tiles using statistical design of mixture experiments. *J Eur Ceram Soc* 2008;28(16):3027–39.
- [19] Dhanapandian S, Gnanavel B. Using granite and marble sawing power wastes in the production of bricks: spectroscopic and mechanical analysis. *Res J Appl Sci, Eng Technol* 2010;2(1):73–86.
- [20] Binici HF, Shah T, Aksogan O, Kaplan H. Durability of concrete made with granite and marble as recycle aggregates. *J Mater Process Technol* 2008;208(1–3):299–308.
- [21] Marmol I, Ballester P, Cerro S, Monros G, Morales J, Sanchez L. Use of granite sludge wastes for the production of coloured cement-based mortars. *Cem Concr Compos* 2010;32(8):617–22.
- [22] Abukersh SA, Fairfield CA. Recycled aggregate concrete produced with red granite dust as a partial cement replacement. *Constr Build Mater* 2011;25(10):4088–94.
- [23] Dong JM, Yu HF, Zhang LM. Study on experimental conditions of hydration methods of determining active magnesium oxide content. *J Salt Lack Res* 2010;18(1):38–41.
- [24] Li ZJ, Chau CK. Influence of molar ratios on properties of magnesium oxychloride cement. *Cem Concr Res* 2007;37(6):866–70.
- [25] Li Y, Yu HF, Dong JM, Qiao HX, Wang MJ. Research progress in deliquescence dehalogenation and efflorescence of magnesium oxychloride. *Bullet Chin Ceram Soc* 2010;29(4):858–65.
- [26] Sugimoto K, Dinnebier RE, Schlecht T. Structure determination of Mg₃(OH)₂Cl·4H₂O (F5 phase) from laboratory powder diffraction data and its

- impact on the analysis of problematic magnesia floors. *Acta Crystallogr Sect B-Struct Sci* 2007;63:805–11.
- [27] Sglavo V, De Genua F, Conci A, Ceccato R, Cavallini R. Influence of curing temperature on the evolution of magnesium oxychloride cement. *J Mater Sci* 2011;46(20):6726–33.
- [28] Bruker. Bruker AXS (2006) TOPAS Bruker AXS Inc, Karlsruhe, Germany; 2006.
- [29] Çelik T, Marar K. Effects of crushed stone dust on some properties of concrete. *Cem Concr Res* 1996;26(7):1121–30.
- [30] Deng DH, Zhang CM. The formation mechanism of the hydrate phases in magnesium oxychloride cement. *Cem Concr Res* 1999;29(9):1365–71.
- [31] Chatterj S. Microstructure of magnesium oxychloride cements. *Nature* 1974;250(5465):443.
- [32] Bilinski H, Matrovic B, Mazuranic C, Zunic TB. The formation of magnesium oxychloride phases in the systems $MgO-MgCl_2-H_2O$ and $NaOH-MgCl_2-H_2O$. *J Am Ceram Soc* 1984;67(4):266–9.
- [33] Misra AK, Mathur R. Magnesium oxychloride cement concrete. *Bull Mater Sci* 2007;30(3):239–46.
- [34] Guettala S, Mezghiche B. Compressive strength and hydration with age of cement pastes containing dune sand powder. *Constr Build Mater* 2011;25(3):1263–9.
- [35] Shen S, Yu H. Characterize packing of aggregate particles for paving materials: particle size impact. *Constr Build Mater* 2011;25(3):1362–8.
- [36] Limeira J, Etxeberria M, Agulló L, Molina D. Mechanical and durability properties of concrete made with dredged marine sand. *Constr Build Mater* 2011;25(11):4165–74.
- [37] Qasrawi H, Shalabi F, Asi I. Use of low CaO unprocessed steel slag in concrete as fine aggregate. *Constr Build Mater* 2009;23(2):1118–25.
- [38] Al-Jabri KS, Al-Saidy AH, Taha R. Effect of copper slag as a fine aggregate on the properties of cement mortars and concrete. *Constr Build Mater* 2011;25(2):933–8.
- [39] Türkmenoğlu AG, Tankut A. Use of tuffs from central Turkey as admixture in pozzolanic cements: assessment of their petrographical properties. *Cem Concr Res* 2002;32(4):629–37.
- [40] Mazuranic C, Bilinski H, Matkovic B. Reaction products in the system $MgCl_2-NaOH-H_2O$. *J Am Ceram Soc* 1982;65(10):523–6.